The Be Phenomenon in Early-Type Stars, IAU Colloquium 175
ASP Conference Series, Vol. 214, 2000
M. A. Smith, H. F. Henrichs, and J. Fabregat, eds.

Non-radial Pulsation Modeling of ω (28) CMa

M. Maintz, Th. Rivinius, S. Tubbesing, B. Wolf

Landessternwarte Königstuhl, Heidelberg, Germany

S. Štefl

Astronomical Institute, Academy of Sciences of the Czech Republic

D. Baade

European Southern Observatory, Garching, Germany

Abstract. Adopting non-radial pulsation (*nrp*) the line profile variability *lpv* of several absorption lines of different ions was modeled for ω (28) CMa. The parameters suggested by Baade (1982) to characterise the pulsation could be confirmed. The pulsation period in the inertial frame was found to be negative, i.e. an actually retrograde mode appears prograde due to the rapid stellar rotation. The line profiles could be reproduced in detail including structures like spikes and ramps. They were identified as velocity effect due to the latitudinal component of the *nrp* velocity field v_ϑ in combination with low inclination i. In spite of small photometric variations (Štefl et al. 1999) the *lpv* of the absorption lines can be explained by *nrp* entirely.

1. Introduction

ω (28) CMa (B3IVe) exhibits the strongest short periodic line profile variability (*lpv*) known among Be stars (Baade 1982: $\mathcal{P} = 1.37$ days). Since the extreme *lpv* might be a signpost to understand the more ordinary cases, ω (28) CMa has attracted major attention in recent years (Harmanec 1998; Štefl et al. 1999 and this volume; Balona et al. 1999 and this volume). Using the *nrp* modeling codes BRUCE and KYLIE by Townsend (1997; see also Rivinius, this volume) the *lpv* of several absorption lines of different ions were modeled in detail for a physically consistent set of pulsational and stellar parameters (Table 1). Flux and line-profile grids calculated using ATLAS 9 and BHT (Gummersbach et al. 1998; see also Rivinius, this volume) were used for the spectral synthesis.

Weak structures like spikes and ramps as described by Balona et al. (1999) for He I 6678 could be reproduced for about 20 spectral lines (cf. Fig. 1 for examples). For the search for the parameters characterising the pulsation of ω (28) CMa negative inertial-frame periods (see below) were taken into account, too. For the modeling 32 spectra obtained in January 1999 with FEROS (Kaufer et al. 1999) at the ESO 1.52 m telescope at La Silla, Chile, were taken for comparison.

Table 1. Adopted stellar parameters for a B3IV star, and adopted pulsational parameters. Additionally shown are a couple of parameters computed from these values

Stellar parameters, adopted	
Polar radius, $R_{\rm polar}$	$6.0\,R_\odot$
Polar temperature, $T_{\rm eff,polar}$	22 000 K
Mass, M	$9\,M_\odot$
Rotation, v	350 km/s
Inclination, i	15°
Stellar parameters, computed	
Rotational period, $\mathcal{P}_{\rm rot}$	1.10 days
Critical period, $\mathcal{P}_{\rm crit}$	0.89 days
Critical velocity, $v_{\rm crit}$	436 km/s
Pulsational parameters, adopted	
l	2
m	+2
$\mathcal{P}_{\rm obs.} = \mathcal{P}_{\rm inert.\ frame}$	−1.37 days
Full Amplitude $A = \lvert v_{\rm max}\rvert$	35 km/s
Pulsational parameters, computed	
$\mathcal{P}_{\rm corot}$	0.92 days
k	2.65
Vertical Amplitude	5.66 km/s
Photometric Amplitude	less than 6 mmag

2. The Pulsational Properties of ω (28) CMa

The measured frequency in the inertial frame

$$\omega_{\rm obs.} = \omega_{\rm corot.} - m\,\Omega_{\rm stell.\ rot.}$$

is usually adopted as positive. However, this frequency will be negative if $\omega_{\rm corot.} < m\Omega_{\rm stell.\ rot.}$. The corotating frequency must be positive because the pulsation on the star itself has to be in the positive direction of time. Then, if a retrograde mode (positive m) is considered and the rotation frequency is high enough, such a mode can appear as prograde *lpv* because of the rapid rotation. For a given observed period of a rapidly rotating star, this may significantly expand the parameter space to be explored to find the appropriate mode.

The *lpv* of ω (28) CMa is not only extreme as such, but can even differ significantly from line to line (Fig. 1). Nevertheless, allowing also for negative inertial-frame periods, one mode was found that reproduces the variations even in detail (Fig. 1) with one and the same set of stellar and pulsational parameters: $l = 2, m = +2$, as suggested by Baade (1982), and $\mathcal{P}_{\rm obs.} = -1.37$. Although the local temperature variations are high (several thousand K) the disk-averaged temperature is constant and the modeled photometric amplitude less than 6 mmag. The radial and horizontal displacements are less than 4 % of the radius and less than 2 % of circumference and therefore acceptably small.

The apparent V/R emission variability with $\mathcal{P} = 1.37$ days can entirely be attributed to the underlying photospheric *nrp* (cf. Fig. 1, Hγ residuals).

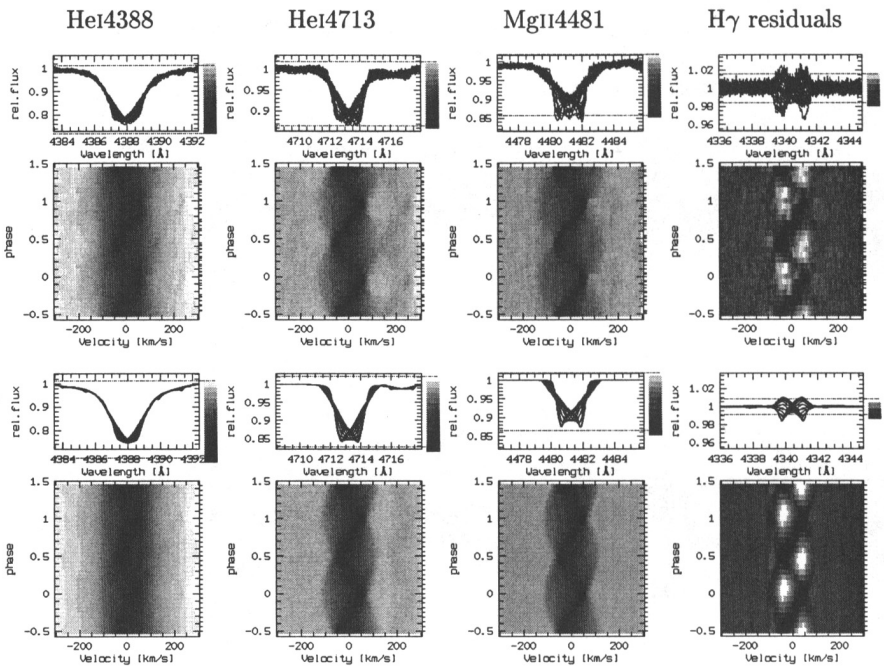

Figure 1. Observed data (upper row) and the *nrp* model (lower row) for four spectral lines. For Hγ the residuals from the mean profiles are shown because of the constant emission contribution in the data. Although all lines are modeled with the same parameter set (Table 1), the differences between the spectral lines are modeled well. The model reproduces the detailed variability seen in the data: variability beyond $v \sin i$ (ramps, at $\phi = 0.5$ and 0), strong spikes ($\phi = 0$ and 0.5), and backward travelling bumps ($\phi = 0.1$ to 0.4). For He I 4388 and 4713 weak FeII lines within the displayed range are modeled as well

3. The Formation of Spikes and Ramps

The presence of spikes and ramps in the models is closely connected to high-amplitude *g*-mode pulsation. As shown in Fig. 2, both features develop at the same phase when the velocity amplitude of the pulsation is high enough.

The spike forms because the percentage of the stellar surface projected into a small velocity range increases strongly with amplitude for the adopted parameters (Fig. 2). While the longitudinal velocity fields (pulsational φ-velocity field and rotation) are projected with $\sin i$, the latitudinal ϑ-velocity field of the pulsation is projected with $\cos i$ and the contrast to the rotational broadening, therefore, increases for low inclination. For the selected parameters $(v_\vartheta \cos i)/(v_{\rm rot} \sin i) \approx 40\,\%$. When $v_\vartheta \cos i$ is maximal and has different sign than $v_{\rm rot} \sin i$, most surface elements on the respective hemisphere have a comparable projected velocity and contribute to the spike. On the respective other

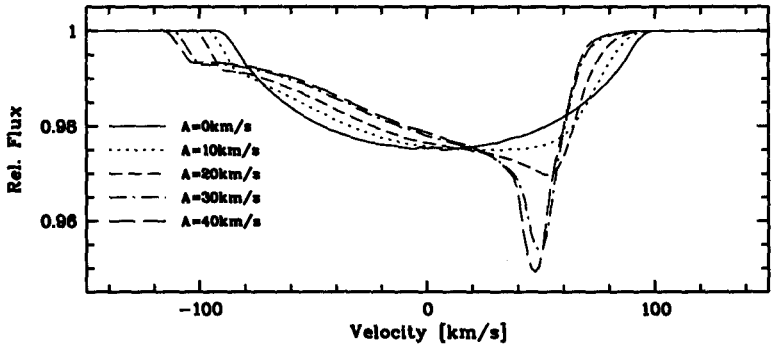

Figure 2. The phase of the red spike occurrence ($\phi = 0$) modeled for different amplitudes A from pure rotation ($A = 0\,\mathrm{km/s}$) to high amplitude pulsation ($A = 40\,\mathrm{km/s}$). Simultaneously an extended ramp develops on the blue side

side of the stellar disk the opposite happens. A small part of the surface is projected into a very large velocity range, including the high-velocity domain, and a ramp extending beyond $v \sin i$ forms.

4. Conclusion

The *lpv* of ω (28) CMa could be modeled in high detail as *nrp*. These details include the far wing variability, the spikes, the backward travelling bumps, and the very low photometric amplitude (Štefl et al. 1999). These results were achieved with generally accepted, general-purpose *nrp*- and atmosphere-models. The patch model proposed by Balona et al. (1999) was by now only applied to He I 6678. It gives a good approximation for the central region of this line, but requires, without physical justification, the *ad hoc* assumption of peculiar variable intrinsic (local) line widths and does not explain the extended ramps. We conclude that ω (28) CMa is a non-radially pulsating Be star and that this property can explain the observed periodic *lpv* ($\mathcal{P} = 1.37\,\mathrm{day}$) entirely.

References

Baade, D. 1982, A&A 105, 65
Balona, L.A., Aerts, C., Štefl, S. 1999, MNRAS 305, 519
Gummersbach, C.A., Kaufer, A., Schäfer, D.R., et al. 1998, A&A 338, 881
Harmanec, P. 1998, A&A 334, 558
Kaufer, A., Stahl, O., Tubbesing, S., et al. 1999, The ESO Messenger 95, 8
Štefl, S., Aerts, C., Balona L.A. 1999, MNRAS 305, 505
Townsend, R.H.D. 1997, MNRAS 284, 839